545-mA/mm E-Mode Recessed-Gate GaN MOSHEMT ($V_{th} > 4$ V) by Ion Beam Etching

Han Gao, Yitian Gu, Yu Zhang, Jialun Li, Junmin Zhou, Haowen Guo, Kei May Lau, *Life Fellow, IEEE*, and Xinbo Zou, *Member, IEEE*

***Abstract*— Normally-off recessed-gate AlGaN/GaN metal–oxide–semiconductor high-electron-mobility transistors (MOSHEMTs) were fabricated using argon-based ion beam etching and thoroughly characterized. By partially recessing the AlGaN barrier, the device achieved a threshold voltage of 4.22 V, saturation drain current of 545 mA/mm, and small on-resistance of 3.63 Ω·mm at a gate bias of 8 V. The recessed-gate MOSHEMT demonstrated good breakdown characteristics that by scaling the gate-to-drain distance (L_{gd}) from 2 μm to 10 μm, breakdown voltages were steadily enhanced from 202 V to 730 V. The device exhibited good dynamic performance that with an off-state drain stressing of 100 V, low current collapse of 14.1% was obtained. After applying a -10 V gate stressing for a duration of 100 s, the threshold voltage was only negatively shifted by 0.40 V. Overall, Baliga's figure-of-merit (FOM) of 567 MW/cm^2 has been achieved for MOSHEMTs with L_{gd} of 10 μm, indicating ion beam etching paves a promising path for enhancement-mode recessed-gate MOSHEMT fabrication.**

***Index Terms*— Enhancement mode, ion beam etching, MOSHEMT, recessed-gate, normally-off.**

I. Introduction

GAN based high electron mobility transistors (HEMTs) are highly desirable for efficient power conversion due to their substantially large forward current and outstanding breakdown performance [1], [2]. In recent years, due to growing concerns regarding the fail-safe design requirement, considerable effort has been devoted to achieving normally-off HEMT devices. Recessed-gate and p-GaN gate are two representative techniques for realization of enhancement-mode devices [3], [4], [5], [6]. Compared to p-GaN gate HEMTs, recessed-gate metal-oxide-semiconductor (MOS) HEMTs opt to be free from hole injection from p-GaN layer and impose fewer requirements on starting epi-structure [7].

Cl-based inductively coupled plasma reactive ion etching (ICP-RIE) has been widely used for recessing AlGaN barrier layer in the gate region [8], [9]. Recently, a threshold voltage (V_{th}) of 4.6 V has been obtained through complete removal of the AlGaN barrier layer [10]. However, plasma-associated damage as well as defects originated from charge repelling or ultraviolet radiation has been commonly observed for devices processed by ICP-RIE [11], [12], [13].

Ion beam etching (IBE) which features a collimated beam of inert gas particles for directional etching of material via physical bombardment holds great potential to realize precise etching and low damage. With a charge neutralizer inside the IBE system, the etching process relies on atom ejection upon neutralized particle impact on the target material. Reduced damage could be well achieved by lowering the ion energy, in addition to absence of charge build-up and repelling [14], [15], [16]. Previously, IBE has been employed for GaN etching to create nearly vertical sidewalls [17], [18]. Recently, IBE technique has been utilized in the fabrication of GaN-based laser diodes [19] and p–i–n diodes [20]. In this work, high-performance recessed-gate MOSHEMT was fabricated with argon-based IBE and thoroughly investigated. The fabricated MOSHEMT exhibited well controlled normally-off operations and low on-resistance. The device demonstrates high breakdown voltage and shows reliable dynamic performance. The findings of this work offer a promising approach for the fabrication of recessed-gate MOSHEMTs, starting from conventional AlGaN/GaN epi-layers.

II. Fabrication of Recessed-Gate MOSHEMT

The recessed-gate AlGaN/GaN MOSHEMT in this study [Fig. 1] was grown on a 6-inch Si by metal-organic chemical vapor deposition (MOCVD). It consisted of AlN/GaN-based buffer layers, a 200 nm channel layer, a 1 nm AlN spacer layer, 15 nm AlGaN barrier layer, and a 2 nm GaN cap layer. After mesa isolation, gate recessing structure was defined by IBE. The energy of incident argon ion during IBE was set to be relatively low (200 eV) to reduce surface roughness

Manuscript received 24 January 2024; revised 8 March 2024; accepted 6 April 2024. Date of publication 9 April 2024; date of current version 23 May 2024. This work was supported in part by ShanghaiTech University Startup Fund under Grant 2017F0203-000-14, in part by the National Natural Science Foundation of China under Grant 52131303, in part by the Natural Science Foundation of Shanghai under Grant 22ZR1442300, and in part by the Chinese Academy of Sciences (CAS) Strategic Science and Technology Program under Grant XDA18000000. The work of Han Gao and Yitian Gu was supported by ShanghaiTech University Quantum Device Laboratory. The review of this letter was arranged by Editor Y. Wu. *(Han Gao and Yitian Gu contributed equally to this work.) (Corresponding author: Xinbo Zou.)*

Han Gao, Junmin Zhou, Haowen Guo, and Xinbo Zou are with the School of Information Science and Technology (SIST), ShanghaiTech University, Shanghai 201210, China (e-mail: zouxb@shanghaitech.edu.cn).

Yitian Gu and Yu Zhang are with the School of Information Science and Technology (SIST), ShanghaiTech University, Shanghai 201210, China, also with the School of Microelectronics, University of Chinese Academy of Sciences, Beijing 101408, China, and also with Shanghai Institute of Microsystem and Information Technology, Shanghai 200050, China.

Jialun Li and Kei May Lau are with the Department of Electronic and Computer Engineering, The Hong Kong University of Science and Technology, Hong Kong.

Color versions of one or more figures in this letter are available at https://doi.org/10.1109/LED.2024.3386824.

Digital Object Identifier 10.1109/LED.2024.3386824

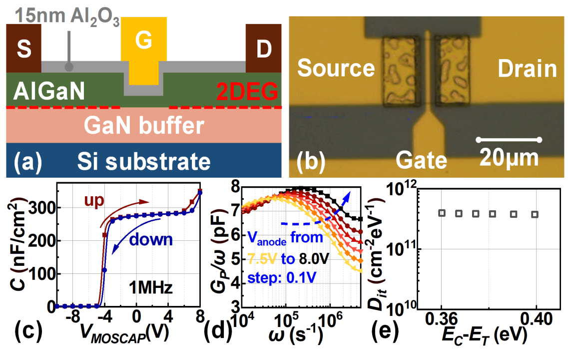

Fig. 1. (a) Schematic and (b) microscopic photograph of the recessed-gate MOSHEMT. (c) Double sweep C–V characteristics of Al_2O_3 MOSCAP at 1 MHz. (d) Parallel conductance as a function of radial frequency with different bias voltages. (e) Interface trap state density with trap energy levels below the conduction band edge.

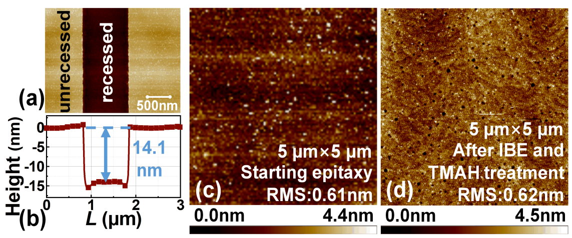

Fig. 2. (a) Trench profile and (b) extracted average height of a 1μm width recessed gate region. 5 μm×5 μm surface morphology of (c) starting epitaxy and (d) the surface following IBE etching and TMAH treatment, measured by AFM.

and mitigate etching damage [14], [21]. The incident argon beam was vertical to the device surface for steep sidewalls and sharp edges. The nominal etching rate for AlGaN layer and etching time for the recessed device are around 3 nm/min and 4.5 minutes, respectively. The ohmic metal stack composed of Ti/Al/Ni/Au (20/150/50/80 nm) was deposited in source and drain regions, followed by rapid thermal annealing at 850 °C for 40 s in a N_2 ambient. 15 nm-thick Al_2O_3 dielectric layer was deposited immediately by plasma-enhanced atomic layer deposition (PEALD) at 300 °C, which also served as a passivation layer for the access regions. Finally, gate and contact pads were formed by Ni/Au (20/200 nm). The gate length L_g, gate-source distance L_{gs}, gate-drain distance L_{gd}, and gate width W_g of the devices were 1 μm, 2 μm, 2 μm, 20 μm, respectively, unless otherwise stated.

III. Results and Discussion

Double sweep capacitance-voltage hysteresis characteristic at 1 MHz of a metal-oxide-semiconductor capacitor (MOSCAP) was plotted in Fig. 1(c). 0.3 V and 0.9V hysteresis were observed for negative gate bias and positive gate bias, respectively. Using parallel conductance method, trap densities were extracted, ranging from 3.95×10^{11} to 3.73×10^{11} cm^{-2}eV^{-1} with trap levels spanning from 0.36 eV to 0.40 eV below the conduction band [Fig. 1(d, e)].

The surface of recessed gate region was characterized by atomic force microscopy (AFM). Fig. 2(a) and Fig. 2(b) showed the trench profile of the recessed gate area with a width of 1μm and depth of 14.1 nm. As shown in Fig. 2(c)-(d), the root-mean-square (RMS) roughness of starting epitaxy and after the ion beam etching process and 5 minutes 60 ° tetramethylammonium hydroxide (TMAH) treatment were 0.61 nm and 0.62 nm, respectively, for a scanned area of 5 μm×5 μm, indicating a highly smooth etching surface achieved by IBE.

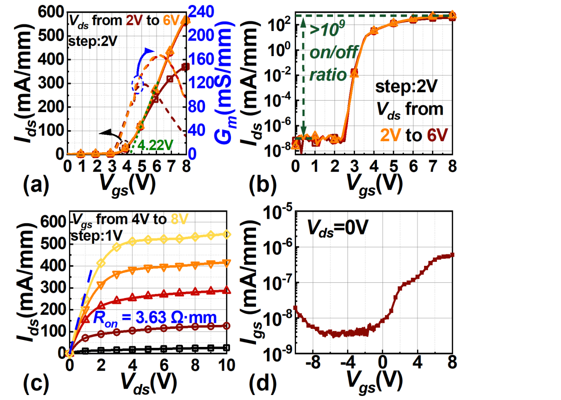

Fig. 3. (a) Linear and (b) log scale transfer characteristics and (c) output characteristics of GaN MOSHEMT. (d) Absolute value of gate leakage current of the normally-off GaN MOSHEMT.

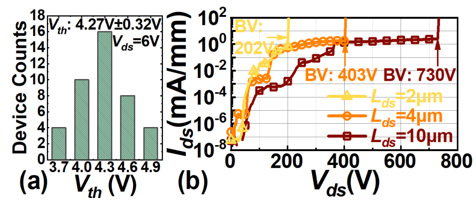

Fig. 4. (a) Threshold voltage uniformity of the fabricated E-mode GaN MOSHEMTs and (b) three terminal off-state breakdown characteristics measured at $V_{gs} = -10$ V for the recessed-gate AlGaN/GaN MOSHEMT.

Fig. 3(a) illustrated transfer characteristics of the normally-off AlGaN/GaN MOSHEMT. The device exhibited a V_{th} of 4.22 V at $V_{ds} = 6$ V, which was determined using a linear extrapolation method. Peak transconductance (G_m) of 168 mS/mm was achieved at $V_{ds} = 6$ V and $V_{gs} = 6.2$ V. The device exhibited good on/off drain current ratio of 3.3×10^9 and relatively low subthreshold slope of 101 mV/dec, as shown in Fig. 3(b). The output characteristics of this device were presented in Fig. 3(c). At $V_{gs} = 8$ V, the recessed MOSHEMT presented a maximum drain current of 545 mA/mm and on-resistance (R_{on}) of 3.63 Ω·mm. The gate leakage current remained a low level of below 20 pA/mm at gate bias of -10 V and 0.6 nA/mm for gate bias of 8 V, as shown in Fig. 3(d). The breakdown voltage of the 15nm PE-ALD Al_2O_3 was measured to be 11.2V, corresponding to an average electric field of 7.5MV/cm.

Fig. 4(a) plotted the V_{th} distribution measured on 42 fabricated devices. The V_{th} showed a narrow distribution with an average value of 4.27 V and a standard deviation of 0.32 V, suggesting excellent etching depth uniformity. Fig. 4(b) showed the off-state breakdown characteristics of normally-off MOSHEMTs with L_{gd} dimensions of 2, 4 and 10 μm. The off-state breakdown voltages were determined to be 202 V, 403 V, and 730 V, respectively, which could be further improved by inclusion of field plate structure.

Dynamic performance of the recessed-gate MOSHEMT was shown in Fig. 5. Pulsed output curves were measured at $V_{gs} = 8$ V with a fixed gate quiescent bias (V_{gsQ}) of 0 V and varied drain quiescent bias (V_{dsQ}) from 0 V to 100 V. The pulse width and pulse period were set at 1 ms and 10 ms, respectively. The current collapse ratio

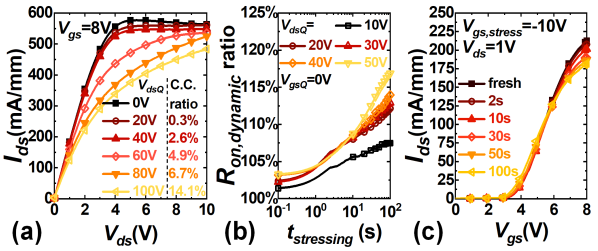

Fig. 5. (a) Pulsed output characteristics. The quiescent drain bias voltage was varied from 0 V to 100 V. (b) Variation of R_{on} as a function of stressing time with various drain quiescent biases at gate quiescent bias of 0 V. (c) Negative bias threshold voltage instability with gate stress of −10 V.

TABLE I
COMPARISON OF STATE-OF-THE-ART RECESSED-GATE GaN MOSHEMTs

Ref.	V_{th} (V)	$I_{DS,\,max}$ (mA/mm)	$R_{on,\,sp}$ (mΩ·cm²)	V_{BR} (L_{gd})	on/off ratio
This work	4.22 4.29	545 450	0.18 0.94	202 V (2 μm) 730 V (10 μm)	10^9
[24]	0.30	581	1.36	1700 V (20 μm)	10^9
[25]	0.50	505	4.17	533 V (15 μm)	10^6
[26]	1.50	693	1.18	860 V (10 μm)	10^8
[27]	2.00	608	1.27	1190 V (10 μm)	10^9
[28]	2.20	519	2.58	1456 V (21 μm)	10^9
[29]	2.37	370	2.44	/	10^8
[30]	2.50	350	4.00	900 V (17 μm)	10^9
[10]	3.50	722	0.39	428 V (7 μm)	/
[31]	6.28	683	2.79	1778 V (20 μm)	10^8

(C.C. ratio) were extracted from the drain currents at V_{ds} of 10V using an expression of 100%-$I_{sat,fresh}/I_{sat,stressed}$. As shown in Fig. 5(a), when subjected to 20 V of drain stressing, the output current was slightly reduced and the degradation percentage of drain current was only 0.3%, measured at $V_{ds} = 10$ V. As the drain quiescent bias was increased, incremental collapse of the maximum drain current was observed. A V_{dsQ} of 100 V would result in a 14.1% current collapse. Fig. 5(b) showed the time-dependent dynamic on-resistance ratio ($R_{on,dynamic}/R_{on,static}$) with off-state drain stressing bias ranging from 10 to 50 V. On-resistances were extracted from the linear region of output curve ($V_{gs} = 8$V and $V_{ds} = 0.5$ V). In the case of $V_{dsQ} = 10$ V, the dynamic R_{on} remained as low as 107% of static value for a stressing time of 100s. When the stressing level and duration of V_{dsQ} was increased to 50V for 100s, the dynamic R_{on} ratio was slightly worsened to 117%. Fig. 5(c) showed time-dependent negative bias-induced threshold voltage instability (NBTI) with a −10 V gate stressing voltage ($V_{gs,stress}$). As $V_{gs,stress}$ of −10 V was applied for 2 s, the threshold voltage was barely shifted. When the stress duration was extended to over 10 s, the threshold voltage shifted gradually in the negative direction. After 100 s of stressing, the V_{th} shift was amounted to −0.40 V and current collapse of 14.2 % was observed. When a negative gate bias was applied to the device, emission of electrons from filled traps in the oxide or at the Al_2O_3/AlGaN interface would lead to a negatively shifted threshold voltage [22], [23].

Table I provided a comparison between the device results of this study and state-of-the-art recessed-gate AlGaN/GaN MOSHEMTs. The threshold voltages listed were obtained using the linear extrapolation method. Fig. 6(a) and Fig. 6(b) illustrated the benchmark of saturation drain current versus threshold voltage and $R_{on,sp}$ versus BV for the recessed-gate AlGaN/GaN MOSHEMT. Zhang et al. [31] reported a recessed device with a V_{th} of 6.28 V, but a high specific on-resistance of 2.79 mΩ·cm² was observed. Zhou et al. [26] demonstrated a high saturation drain current of 693 mA/mm, but the threshold voltage was relatively small. In this study, well-balanced device performance was simultaneously obtained including a threshold voltage of 4.22 V and a sufficiently high saturation current of 545 mA/mm. The device achieved $R_{on,sp}$of 0.18 mΩ·cm² and 202 V breakdown voltage for 2 μm gate-drain distance. Extending gate-drain distance to 10 μm greatly improved breakdown voltage to 730V while remained relatively-small specific on-resistance of 0.94 mΩ·cm². Baliga's figure-of-merit (FOM) of 227 MW/cm² and 567 MW/cm² were acquired for MOSHEMTs with L_{gd} of 2 μm (solid) and 10 μm (hollow), respectively. Additionally, the recessed-gate MOSHEMT fabricated using the argon-based ion beam etching technique exhibited good breakdown endurance, superior on/off current ratio, and outstanding dynamic reliability.

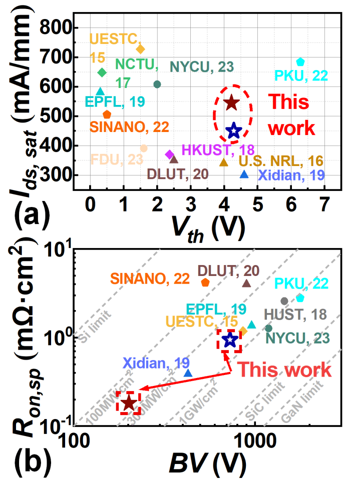

Fig. 6. Benchmark of (a) $I_{ds,\,sat}$ versus V_{th} and (b) $R_{on,sp}$ versus BV for state-of-the-art recessed-gate AlGaN/GaN MOSHEMTs. Solid and hollow stars represented devices with L_{gd} of 2 μm and 10 μm.

IV. CONCLUSION

High performance normally-off recessed-gate AlGaN/GaN MOSHEMT was implemented by an argon-based IBE method. The IBE features a precise control of AlGaN barrier removal and a smooth etched surface. The device demonstrated a threshold voltage of 4.22 V, a saturation current of 545 mA/mm, and a low specific on-resistance of 0.18 mΩ·cm². On/off current ratio of 10^9 and a high breakdown voltage of 730 V were also achieved. The recessed-gate MOSHEMT exhibited stable dynamic performance, with a low 14.1% current collapse with a V_{dsQ} of 100 V and a 117% increase in dynamic on-resistance with 100 s V_{dsQ} of 50 V. Additionally, a V_{th} shift of −0.40 V was observed upon a 100 s stressing at −10 V gate bias. 567 MW/cm² FOM were obtained for recessed-gate MOSHEMTs with L_{gd} of 10 μm. These results highlight that IBE gate recessing offers a promising approach for the fabrication of high-performance normally-off GaN MOSHEMTs to be used in power applications.

References

[1] T. Oka and T. Nozawa, "AlGaN/GaN recessed MIS-gate HFET with high-threshold-voltage normally-off operation for power electronics applications," *IEEE Electron Device Lett.*, vol. 29, no. 7, pp. 668–670, Jul. 2008, doi: 10.1109/LED.2008.2000607.

[2] Z. Tang, Q. Jiang, Y. Lu, S. Huang, S. Yang, X. Tang, and K. J. Chen, "600-V normally off SiN_x/AlGaN/GaN MIS-HEMT with large gate swing and low current collapse," *IEEE Electron Device Lett.*, vol. 34, no. 11, pp. 1373–1375, Nov. 2013, doi: 10.1109/LED.2013.2279846.

[3] M. Hua, J. Wei, G. Tang, Z. Zhang, Q. Qian, X. Cai, N. Wang, and K. J. Chen, "Normally-off LPCVD-SiN_x/GaN MIS-FET with crystalline oxidation interlayer," *IEEE Electron Device Lett.*, vol. 38, no. 7, pp. 929–932, Jul. 2017, doi: 10.1109/LED.2017.2707473.

[4] J. Zhou, H. Guo, H. Du, Y. Zhang, H. Qu, W. Huang, J. Zhou, Z. Xiao, and X. Zou, "RF p-GaN HEMT with 0.9-dB noise figure and 12.8-dB associated gain for LNA applications," *IEEE Electron Device Lett.*, vol. 44, no. 9, pp. 1412–1415, Sep. 2023, doi: 10.1109/LED.2023.3294696.

[5] M. Sun, L. Wang, P. Zhang, and K. Chen, "Improving performance of Al_2O_3/AlN/GaN MIS HEMTs via in situ N_2 plasma annealing," *Micromachines*, vol. 14, no. 6, p. 1100, May 2023, doi: 10.3390/mi14061100.

[6] Y. C. Lin, Y. X. Huang, G. N. Huang, C. H. Wu, J. N. Yao, C. M. Chu, S. Chang, C. C. Hsu, J. H. Lee, K. Kakushima, K. Tsutsui, H. Iwai, and E. Y. Chang, "Enhancement-mode GaN MIS-HEMTs with $LaHfO_x$ gate insulator for power application," *IEEE Electron Device Lett.*, vol. 38, no. 8, pp. 1101–1104, Aug. 2017, doi: 10.1109/LED.2017.2722002.

[7] M. Hua, Z. Zhang, J. Wei, J. Lei, G. Tang, K. Fu, Y. Cai, B. Zhang, and K. J. Chen, "Integration of LPCVD-SiN_x gate dielectric with recessed-gate E-mode GaN MIS-FETs: Toward high performance, high stability and long TDDB lifetime," in *IEDM Tech. Dig.*, Dec. 2016, pp. 10.4.1–10.4.4, doi: 10.1109/IEDM.2016.7838388.

[8] H.-Y. Liu, C.-W. Lin, W.-C. Hsu, C.-S. Lee, M.-H. Chiang, W.-C. Sun, S.-Y. Wei, and S.-M. Yu, "Integration of gate recessing and in situ Cl-doped Al_2O_3 for enhancement-mode AlGaN/GaN MOSHEMTs fabrication," *IEEE Electron Device Lett.*, vol. 38, no. 1, pp. 91–94, Jan. 2017, doi: 10.1109/LED.2016.2625304.

[9] T. J. Anderson, V. D. Wheeler, D. I. Shahin, M. J. Tadjer, A. D. Koehler, K. D. Hobart, A. Christou, F. J. Kub, and C. R. Eddy, "Enhancement mode AlGaN/GaN MOS high-electron-mobility transistors with ZrO_2 gate dielectric deposited by atomic layer deposition," *Appl. Phys. Exp.*, vol. 9, no. 7, Jul. 2016, Art. no. 071003, doi: 10.7567/apex.9.071003.

[10] Y. He, H. Gao, C. Wang, Y. Zhao, X. Lu, C. Zhang, X. Zheng, L. Guo, X. Ma, and Y. Hao, "Comparative study between partially and fully recessed-gate enhancement-mode AlGaN/GaN MIS HEMT on the breakdown mechanism," *Phys. Status Solidi A*, vol. 216, no. 16, Aug. 2019, Art. no. 1900115, doi: 10.1002/pssa.201900115.

[11] S. Samukawa, "Ultimate top-down etching processes for future nanoscale devices: Advanced neutral-beam etching," *Japanese J. Appl. Phys.*, vol. 45, no. 4R, p. 2395, Apr. 2006, doi: 10.1143/jjap.45.2395.

[12] Y.-K. Lin, S. Noda, H.-C. Lo, S.-C. Liu, C.-H. Wu, Y.-Y. Wong, Q. H. Luc, P.-C. Chang, H.-T. Hsu, S. Samukawa, and E. Y. Chang, "AlGaN/GaN HEMTs with damage-free neutral beam etched gate recess for high-performance millimeter-wave applications," *IEEE Electron Device Lett.*, vol. 37, no. 11, pp. 1395–1398, Nov. 2016, doi: 10.1109/LED.2016.2609938.

[13] Y.-K. Lin, S. Noda, C.-C. Huang, H.-C. Lo, C.-H. Wu, Q. H. Luc, P.-C. Chang, H.-T. Hsu, S. Samukawa, and E. Y. Chang, "High-performance GaN MOSHEMTs fabricated with ALD Al_2O_3 dielectric and NBE gate recess technology for high frequency power applications," *IEEE Electron Device Lett.*, vol. 38, no. 6, pp. 771–774, Jun. 2017, doi: 10.1109/LED.2017.2696569.

[14] V. Chulukhadze, K. Huynh, J. Kramer, M. Liao, S. Cho, L. Matto, O. A. Barrera, C. Cui, M. S. Goorsky, and R. Lu, "Frequency scaling millimeter wave acoustic resonators using ion beam trimmed lithium niobate," in *Proc. Joint Conf. Eur. Freq. Time Forum IEEE Int. Freq. Control Symp. (EFTF/IFCS)*, May 2023, pp. 1–4, doi: 10.1109/EFTF/IFCS57587.2023.10272038.

[15] R. James, Y. Pilloux, and H. Hegde, "Reactive ion beam etching of piezoelectric ScAlN for bulk acoustic wave device applications," *J. Phys., Conf. Ser.*, vol. 1407, no. 1, Nov. 2019, Art. no. 012083, doi: 10.1088/1742-6596/1407/1/012083.

[16] P. F. P. P. Rocha, L. Vauche, P. Pimenta-Barros, S. Ruel, R. Escoffier, and J. Buckley, "Recent developments and prospects of fully recessed MIS gate structures for GaN on Si power transistors," *Energies*, vol. 16, no. 7, p. 2978, Mar. 2023, doi: 10.3390/en16072978.

[17] I. Adesida, A. T. Ping, C. Youtsey, T. Dow, M. A. Khan, D. T. Olson, and J. N. Kuznia, "Characteristics of chemically assisted ion beam etching of gallium nitride," *Appl. Phys. Lett.*, vol. 65, no. 7, pp. 889–891, Aug. 1994, doi: 10.1063/1.112191.

[18] A. T. Ping, I. Adesida, and M. A. Khan, "Study of chemically assisted ion beam etching of GaN using HCl gas," *Appl. Phys. Lett.*, vol. 67, no. 9, pp. 1250–1252, Aug. 1995, doi: 10.1063/1.114387.

[19] L. Y. Kuritzky, D. L. Becerra, A. S. Abbas, J. Nedy, S. Nakamura, S. P. DenBaars, and D. A. Cohen, "Chemically assisted ion beam etching of laser diode facets on nonpolar and semipolar orientations of GaN," *Semicond. Sci. Technol.*, vol. 31, no. 7, Jul. 2016, Art. no. 075008, doi: 10.1088/0268-1242/31/7/075008.

[20] D. V. Smirnov, K. O. Boltar, M. V. Sednev, and Y. P. Sharonov, "Characteristics of heteroepitaxial structures $Al_xGa_{1-x}N$ for $p-i-n$ diode focal plane arrays," *J. Commun. Technol. Electron.*, vol. 61, no. 3, pp. 358–362, Mar. 2016, doi: 10.1134/s1064226916030189.

[21] R. M. R. Pinto, V. Gund, C. Calaza, K. K. Nagaraja, and K. B. Vinayakumar, "Piezoelectric aluminum nitride thin-films: A review of wet and dry etching techniques," *Microelectronic Eng.*, vol. 257, Mar. 2022, Art. no. 111753, doi: 10.1016/j.mee.2022.111753.

[22] A. Guo and J. A. del Alamo, "Negative-bias temperature instability of GaN MOSFETs," in *Proc. IEEE Int. Rel. Phys. Symp. (IRPS)*, Apr. 2016, pp. 4A-1-1-4A-1-6, doi: 10.1109/IRPS.2016.7574526.

[23] F. Sang, M. Wang, C. Zhang, M. Tao, B. Xie, C. P. Wen, J. Wang, Y. Hao, W. Wu, and B. Shen, "Investigation of the threshold voltage drift in enhancement mode GaN MOSFET under negative gate bias stress," *Jpn. J. Appl. Phys.*, vol. 54, no. 4, Apr. 2015, Art. no. 044101, doi: 10.7567/jjap.54.044101.

[24] M. Zhu, J. Ma, L. Nela, C. Erine, and E. Matioli, "High-voltage normally-off recessed tri-gate GaN power MOSFETs with low on-resistance," *IEEE Electron Device Lett.*, vol. 40, no. 8, pp. 1289–1292, Aug. 2019, doi: 10.1109/LED.2019.2922204.

[25] W. Liu, G. Yu, J. Zhou, Z. Yu, X. Wei, W. Tang, L. Zhang, and B. Zhang, "Implementation of recessed gate normally off GaN metal–insulator–semiconductor high electron mobility transistors by electrodeless photoelectrochemical etching," *ACS Appl. Electron. Mater.*, vol. 4, no. 3, pp. 897–902, Mar. 2022, doi: 10.1021/acsaelm.1c01267.

[26] Q. Zhou, B. Chen, Y. Jin, S. Huang, K. Wei, X. Liu, X. Bao, J. Mou, and B. Zhang, "High-performance enhancement-mode Al_2O_3/AlGaN/GaN-on-Si MISFETs with 626 MW/cm^2 figure of merit," *IEEE Trans. Electron Devices*, vol. 62, no. 3, pp. 776–781, Mar. 2015, doi: 10.1109/TED.2014.2385062.

[27] A.-C. Liu, P.-T. Tu, H.-C. Chen, Y.-Y. Lai, P.-C. Yeh, and H.-C. Kuo, "Improving performance and breakdown voltage in normally-off GaN recessed gate MIS-HEMTs using atomic layer etching and gate field plate for high-power device applications," *Micromachines*, vol. 14, no. 8, p. 1582, Aug. 2023, doi: 10.3390/mi14081582.

[28] Q. Hu, S. Li, T. Li, X. Wang, X. Li, and Y. Wu, "Channel engineering of normally-OFF AlGaN/GaN MOS-HEMTs by atomic layer etching and high-κ dielectric," *IEEE Electron Device Lett.*, vol. 39, no. 9, pp. 1377–1380, Sep. 2018, doi: 10.1109/LED.2018.2856934.

[29] J. He, M. Hua, Z. Zhang, and K. J. Chen, "Performance and VTH stability in E-mode GaN fully recessed MIS-FETs and partially recessed MIS-HEMTs with LPCVD-SiN_x/PECVD-SiN_x gate dielectric stack," *IEEE Trans. Electron Devices*, vol. 65, no. 8, pp. 3185–3191, Aug. 2018, doi: 10.1109/TED.2018.2850042.

[30] Z. Sun, H. Huang, R. Wang, N. Sun, P. Tao, Y. Ren, S. Song, H. Wang, S. Li, W. Cheng, J. Gao, and H. Liang, "Improving performances of enhancement-mode AlGaN/GaN MIS-HEMTs on 6-inch Si substrate utilizing SiON/Al_2O_3 stack dielectrics," *IEEE Electron Device Lett.*, vol. 41, no. 1, pp. 135–138, Jan. 2020, doi: 10.1109/LED.2019.2957376.

[31] B. Zhang, J. Wang, X. Wang, C. Wang, C. Huang, J. He, M. Wang, J. Mo, Y. Hu, and W. Wu, "Improved performance of fully-recessed high-threshold-voltage GaN MIS-HEMT with in situ H_2/N_2 plasma pretreatment," *IEEE Electron Device Lett.*, vol. 43, no. 7, pp. 1021–1024, Jul. 2022, doi: 10.1109/LED.2022.3179136.